Quantifying Ventilatory Control Contribution to Sleep Apnoea Using Polysomnography

Online Supplement

Philip Terrill[1,2], Bradley A Edwards[1], Shamim Nemati[1], James P Butler[1], Robert L Owens[1], Danny J Eckert[1,3], David P White[1], Atul Malhotra[1,4], Andrew Wellman[1], Scott A Sands[1,5*]

[1]Division of Sleep Medicine, Brigham and Women's Hospital and Harvard Medical School, Boston, USA; [2]School of Information Technology and Electrical Engineering, The University of Queensland, St. Lucia, Australia; [3]Neuroscience Research Australia (NeuRA) and the School of Medical Sciences, University of New South Wales, Australia. [4]Division of Pulmonary and Critical Care, University of Southern California San Diego, La Jolla, USA; [5]Central Clinical School, The Alfred and Monash University, Melbourne, Australia.

SUPPLEMENTAL THEORY

For the purpose of the current study, the primary interest is 'dynamic' loop gain, which ultimately determines control system stability. Dynamic loop gain refers to the concept that the size of the feedback response depends on the timing or frequency of the disturbance (see Figure S1). Our method provides a measure of loop gain across a range of frequencies. For the purposes of validation, we have chosen to compare loop gain across patients at a common frequency. For simplicity, and for consistency with our previous report of "dynamic" loop gain [1], we chose to focus primarily on loop gain measured at 1 cycle/minute (LG_1; "mid frequency" loop gain). Note that 1 cycle/min is the typical cycling frequency of Cheyne-Stokes respiration. We also present "high frequency" loop gain values (2 cycles/minute, LG_2; typical of idiopathic central sleep apnoea), and "low frequency" values (1 cycle per 6 min, $LG_{1/6}$) to illustrate that loop gain can be measured effectively across a broad physiological range. There are several further points to consider: First, the natural frequency of the control system, in patients with obstructive sleep apnoea (OSA) at sea level, lies roughly between 1-2 cycles/min [2, 3]; see also Table S1. An elevated loop gain measured at the frequency relevant for periodic breathing (1-2 cycles/min; mid-high frequencies) reflects reduced stability and a greater propensity for periodic breathing. Second, elevated "low frequency" loop gain will provide a more vigorous increase in ventilatory drive in response to a long-term reduction in ventilation (e.g. persistent airflow limitation), which can ultimately prevent stable sleep by promoting arousal [4, 5]. We calculate "low frequency" loop gain at 1/6 cycles/min (corresponding to a cycling period of 6 min) as the lowest frequency that can be measured using the window length chosen (slightly under 7 min once accounting for the range of possible delays).

Estimating Loop Gain During Obstructive Sleep Apnoea

As described in the main document, we consider that the overall ventilatory drive (V_{drive}) is the combined effect of increased *chemical drive* (V_{chem}) as a consequence of elevated CO_2 and depleted O_2 [1, 4], and the independent (non-chemical) increase in ventilation that occurs with arousal ($V_{arousal}$) when the 'wakefulness drive' to breathe is reinstated [6-10]:

$$V_{drive}=V_{chem}+V_{arousal} \quad \text{(Equation 1)}$$

Previous studies [4, 11-13] have shown that the rise in chemical drive during obstruction can be adequately encapsulated by a first order time delay system with a circulatory delay (δ), time-constant (τ) and the steady state loop gain (LG_0), as illustrated in Figure 1a (in the main body of the manuscript). The equation relating changes in chemical drive to prior changes in ventilation is given by:

$$\tau\frac{dV_{chem}}{dt} = -V_{chem} - LG_0 V_E(t-\delta) \quad \text{(Equation 2)}$$

Of note, V_{chem} and V_E represent the changes from baseline (mean) levels; thus, $dV_{chem}/dt=0$ when V_{chem} and $V_E(t-\delta)$ are both at their baseline levels. To handle discrete breath-breath data, we re-express Equation 2 to describe the current level of V_{chem} (at breath n) as a function of previous values of V_{chem} (at breath n−1) and previously measured ventilation (V_E):

$$V_{chem}[n]=\alpha V_{chem}[n-1]+\beta V_E^*[n] \quad \text{(Equation S1)}$$

where V_E^* is the "delayed ventilation" (the value of ventilation accounting for a delay [δ]), and α and β are functions of LG_0, τ, and the previous breath duration T_{n-1}:

$$\alpha = \frac{\left(\frac{\tau / T_{n-1}}{1 + \tau / T_{n-1}} + 1 - \frac{T_{n-1}}{\tau} \right)}{2} \quad \text{(Equation S2)}$$

$$\beta = -LG_0 \frac{\left(\frac{1}{1 + \tau / T_{n-1}} + \frac{1}{\tau / T_{n-1}} \right)}{2} \quad \text{(Equation S3)}$$

Thus, α and β are used to determine V_{chem} at breath n; we chose to employ the average of the forward and backwards Euler approximations for α and β as these provided improved accuracy for loop gain measurement (verified using mathematical modeling). Specifically, Equations S1−S3 are found by examining the following discrete forms of Equation 2. The difference equation in 'forward Euler' form is given by:

$$\tau \frac{V_{chem}[n] - V_{chem}[n-1]}{T_{n-1}} = -V_{chem}[n-1] - LG_0 \times V_E^*[n]$$

and the 'backward Euler' form is given by:

$$\tau \frac{V_{chem}[n] - V_{chem}[n-1]}{T_{n-1}} = -V_{chem}[n] - LG_0 \times V_E^*[n]$$

Rearranging these equations provide values of α and β (see Equation S1). Note also that T_{n-1} represents the actual duration of each previous breath (n−1) which is not assumed to be constant. We do not assume an equispaced breath-to-breath series of ventilation data because, occasionally, breath duration can be highly variable during cyclic OSA. By accounting for a variable breath duration, the modeled rise in V_{chem} during a hypopnoea, from one breath to the next, will be smaller for shorter breaths than for longer breaths, as appropriate. Hence, for any chosen set of parameter values (LG_0 and τ), α and β vary with each breath according to changes in T_{n-1}.

Based on Equations S1-S3, we note that V_{chem} is completely determined from measured V_E and the ventilatory chemoreflex parameters; thus knowing these parameters enables the calculation of V_{chem}.

To determine $V_{arousal}$ (the ventilatory response to arousal) we incorporate an additional parameter γ that describes the extra ventilation that is seen during a scored EEG arousal, independent of chemical drive [6, 13-17]. For each breath n we determine whether there is a scored arousal present, Ar[n]=1, or not, Ar[n]=0, such that $V_{arousal}$ is simply given by:

$$V_{arousal}[n] = \gamma Ar[n] \quad \text{(Equation S4)}$$

That is, during an arousal we have $V_{arousal}=\gamma$, otherwise $V_{arousal}=0$. Combining Equation S1 with Equation 1, expressed in the discrete breath domain as $V_{drive}[n]=V_{chem}[n]+V_{arousal}[n]$, we can express overall ventilatory drive (V_{drive}) as:

$$V_{drive}[n] = \alpha V_{chem}[n-1] + \beta V_E^*[n] + \gamma Ar[n] \quad \text{(Equation S5)}$$

To calculate "delayed ventilation", $V_E^*[n]$, for use in Equation S5, we time-shifted the values of $V_E[n]$ by δ (in seconds). However, this delay may correspond to a time that is part-way between breaths. Consider, for example, an estimated delay of δ=8 s, where the previous breath duration, $T_{tot}[n-1]$, is 6 s and the one before that, $T_{tot}[n-2]$, is 4 s. In this case, the ventilation 8 s back from breath n would be a value that lies partway between the two breaths n−1 and n−2. To find $V_E^*[n]$ in these cases, we linearly interpolated between values of $V_E[n]$. For this example, the value of $V_E^*[n]$ would be taken as the value of $V_E[n]$ exactly midway between breaths n−1 and n−2 i.e. $V_E^*[n]=(V_E[n-1]+V_E[n-2])/2$.

Parameter fitting procedure. For a given period of observed ventilation V_E, it is now possible to identify the set of parameters LG_0, τ, δ and γ that provide a V_{drive} trace that best matches V_E during periods of unobstructed breathing. The rationale is that during unobstructed breaths, when the respiratory mechanics are normal, the observed ventilation directly expresses the ventilatory drive ('intended' ventilation based on chemical drive and arousal state). By contrast, during obstructed breaths, observed ventilation is reduced below ventilatory drive; that is, actual ventilation is less than the 'intended' level.

In summary, to best fit V_{drive} (model output) to the ventilation data we employed a typical constrained, weighted least-squares technique. We started by guessing an initial set of parameter values, then Equation S5 was used to convert V_E and arousal data (inputs) into a series of V_{drive} data (output). V_{drive} was then compared to the observed V_E data; the difference between V_{drive} and V_E was calculated for all breaths when the airway was open (by weighting breaths with zero that were scored as obstructive) to provide a series of residuals ('Error'). A further polynomial (third-order) was fit to, and subtracted from, this Error signal (unobstructed breaths only) to reduce contributions of long-term drift and account for non-Gaussian noise (discussed below). Finally the sum of squares of this drift-corrected Error was calculated to determine the adequacy of the parameter values. Adjusting the parameters and recalculating V_{drive} from the model was performed repetitively to find the best set of parameters (i.e. the set of parameters which minimised the sum of squares of the drift-corrected error). Parameters were constrained within reasonable limits, including constraints that gain and delay values remain positive. Details are described as follows:

First, we provided the model with a starting (initial) value of chemical drive at the beginning of the epoch (time=0; breath n=0), denoted $V_{chem}[0]$. This initial estimate of V_{chem} is required in order to calculate subsequent values of V_{chem} (and thus V_{drive}), which is clear from Equations S1 and S5. Mathematically, $V_{chem}[0]$ can be described as the addition of the observed ventilation at time=0 ($V_E[0]$) and an initial difference between the estimated V_{chem} and the observed V_E (i.e. due to airflow obstruction or model error). This difference, referred to as Error[0], is the 5th and final parameter that was estimated in the fitting algorithm.

Given a starting parameter set, the model (Equation S5) was 'run' in order to calculate V_{drive} at each breath from the V_E data. Comparing V_{drive} with V_E yields the residuals or 'Error' of the model for each breath n, whereby:

$$Error[n]=V_E[n]-V_{drive}[n] \qquad \text{(Equation S6)}$$

To deal with non-stationarity (e.g. drifting baseline ventilation) and non-Gaussian (non-white) noise, we subtracted a (zero-meaned) third-order polynomial P[n] from the model Error (Equation S6), thereby removing the effect of long-term drift: $Error^*[n]=Error[n]-P[n]$. By minimizing effects of non-stationarity we were able to maximise the window width (7 min).

Moreover, subtracting low-frequency error/noise from the measurement enables the best-fit to focus on the higher-frequency dynamics that are of primary interest for ventilatory control stability. Of note, we observed no detrimental effect of this procedure on loop gain measurement using the mathematical model.

Ultimately, the strength of the chosen set of parameters (LG_0, τ, δ, γ and Error[0]) was based on the weighted (normalised) sum of squared residuals (SS_{res}):

$$SS_{res} = \frac{1}{N}\sum_{n=1}^{N} W[n] \cdot \left(Error^{*}[n]\right)^2 \qquad \text{(Equation S7)}$$

where the set of weights W[n] describes whether V_E can be expected to reflect V_{drive} or not for each individual breath (i.e. the squared error for each breath is multiplied by the weight for that breath; the weighted errors are then added up), and N is the number of breaths analyzed in the 7 min epoch. Specifically, W[n] (either 1 or 0) describes whether each breath n is unobstructed (W[n]=1, thus V_E should reflect V_{drive}) or obstructed (W[n]=0, thus V_E is not expected to equal V_{drive}). It is this very weighting procedure that allowed us to use spontaneous breathing to derive measures of ventilatory control from OSA patterns, since the procedure can avoid fruitless attempts to fit ventilatory drive to ventilatory data during obstructed breaths (there is no expectation that ventilatory drive is equal to ventilation at this time).

Another case where V_E is not expected to equal V_{drive} is during central apnoea. During such times, V_{drive} is below zero (e.g. CO_2 below the apneic threshold) [12, 18] and consequently the observed ventilation is zero. To avoid an unreasonable penalty, W[n] is taken as 0 during central apnoea so long as the estimated V_{drive} is below 0 (i.e. conditional weighting).

To ensure that the parameter values were within possible physiological limits, we applied the following constraints: $0.1<LG_0<30$, $2<\tau<180$ s, $T_{tot}<\delta<5T_{tot}$ (T_{tot} is the average breath duration), $0<\gamma<3$ (normalised units where mean $V_E=1$), $-3<Error[0]<3$ (normalised units where mean $V_E=1$). For example, a value of $\gamma=3$ describes a response that is 300% of mean ventilation (~20 l/min).

The model fitting procedure was implemented using a standard (interior point) algorithm (MATLAB; Mathworks, Natick, MA). In essence, parameters are input to the model, which is 'run' (stepping through each breath n to calculate V_{drive}) to determine the *cost* (SS_{res}) associated with the parameters used. The algorithm then adjusts iteratively the parameters such that SS_{res} is

progressively minimised. To maximise the robustness of this procedure (and avoid local minima), a set of five starting conditions (initial parameter values) were applied that spanned the range of allowable values; the starting set that yielded the least SS_{res} (Equation S7) was then identified and the final parameters reached were used as the starting point for further iterations to fine-tune the model. For each epoch, this minimisation procedure was performed separately for each of 5 possible values of delay ($\delta=T_{tot}\times1$, $T_{tot}\times2$, ... $T_{tot}\times5$), as recommended previously [19]. The value of δ that yielded the smallest SS_{res} was chosen, and the best parameters (LG_0, τ, γ) found using this delay were taken to estimate loop gain.

Determining loop gain. The resultant chemoreflex parameters (LG_0, τ and δ) can then be used to determine loop gain via Equation S8, which represents the frequency domain transformation of Equation 2. Loop gain at any frequency *f* (cycles per minute) is given by:

$$LG_f = \frac{\tilde{V}_{chem}}{\tilde{V}_E} = \frac{-LG_0}{1+s\tau} e^{-s\delta} \qquad \text{(Equation S8)}$$

where $s=i2\pi f$, LG_f describes the magnitude (response/disturbance ratio) and phase lag (response-disturbance delay) at each frequency *f*, $i=(-1)^{0.5}$ denotes the part of the chemical feedback response that is 90º 'out of phase' with the swings in ventilation, $\tilde{V}_{chem}$ and $\tilde{V}_E$ denote the frequency-domain representations of V_{chem} and V_E. The natural cycling period (T_n, e.g. periodic breathing cycle duration) is found by finding the lowest value of *f* at which the phase of $LG_f = 0$ (Equation S8); T_n is the reciprocal of this frequency ($T=1/f$) and reflects the period at which the system naturally tends to oscillate if unstable. T_n also reflects the briskness of the control system response, since both a longer delay and greater time-constant will increase T_n.

The MATLAB function to calculate loop gain from a 7-min epoch of ventilation data (with associated arousal and obstructive event scoring) is provided in the MATLAB file "FindBestModelParameters.m", which, in turn, uses the file "TheModel.m". These files include extensive commenting to further detail the specific implementation of the method.

SUPPLEMENTAL METHODS

Computational Model Verification

In order to verify the underlying theory for the measurement of loop gain in OSA, a simplified computational simulation of OSA was implemented (wherein actual loop gain is known precisely) and loop gain was estimated using our method. The model used to simulate OSA exhibited the same 3-parameter structure assumed by our method, thereby allowing us to validate the effectiveness of our approach under ideal conditions. The ventilatory control model is well known [1, 4, 11, 18, 20, 21] and consists of a single homogenous lung compartment for gas exchange, a linear controller, and circulatory delay (parameterised with a lung washout time constant τ_{lung}, delay δ, and steady-state loop gain LG_0). There is one notable non-linearity in the model: ventilation is not permitted to be negative; chemical drive can fall below zero (i.e. as CO_2 falls below the threshold for apnoea) but ventilation cannot [12, 18, 20]. Three types of ventilatory disturbances were provided to simulate the characteristic physiology of OSA: (a) partial reductions in ventilation (hypopnoeas) due to obstructive respiratory events; (b) increased ventilation due to arousal; and (c) random physiological fluctuations in ventilation (white noise) that are unrelated to chemical drive or arousal effects. Respiratory events of random duration (≥3 breaths) were randomly imposed by doubling resistance, which was modeled by halving the controller slope (and maintaining a constant controller intercept). This increase in resistance was employed in a graduated manner over 4 breaths to mimic OSA patterns. Likewise, simulated arousals were provided for 2 breaths to mimic typical clinical data. Additional model parameter values were as follows: delay=12 s, lung washout time constant=12.5 s (based on typical values for lung volume, cardiac output, and alveolar ventilation), probability of arousals at the end of events = 80%, probability of spontaneous arousal on any simulated breath=1%, ventilatory response to arousal γ=0.4 (40% of eupneic ventilation), breath duration =3.5 s. Of note, the effectiveness of the method did not rely on these specific chosen parameters. The random (white noise) variability in ventilatory drive was incorporated with SD=1% of eupneic ventilation.

To vary loop gain we altered the slope of the ventilatory response to carbon dioxide (chemosensitivity or CO_2 controller gain) such that LG_1 varied from 0 to 2 in 100 steps. The 'measured' LG_1 based on the ventilatory pattern of OSA was then compared with the true value of LG_1 given to the model (based on the model parameters).

Simulations were performed in MATLAB (Mathworks, Natick MA, USA). The script used to perform the model analysis is provided in the MATLAB file "ModelSimulation.m". This script uses the functions "FindBestModelParameters.m" and "TheModel.m" (mentioned above) to estimate loop gain from the simulated ventilation data.

Loop Gain Quantification in OSA: Comparison to Published Standard

We examined 28 patients who were a subset of a larger physiological investigation. All patients with apnoea-hypopnoea index [AHI] ≥15 events/h during supine non-REM, and who were studied at our affiliated clinical laboratory (former Sleep Health Centers, MA) were included in our analysis. A flowchart detailing the selection of patients for analysis in this study is provided in Figure S2. Patients were studied on three nights approximately 1 week apart. First, an attended diagnostic clinical polysomnographic study was performed which included measures of electroencephalogram (EEG), electrooculargram, chin electromyogram, snoring sounds, oronasal

airflow (nasal pressure, thermistor), respiratory movements (chest and abdominal belts), pulse oximetry (finger), and position sensor. Sleep stages, EEG arousals (>3 s), and respiratory events were manually scored by an accredited sleep scientist according to standard criteria. Hypopnoeas were defined as events with a >30% reduction in airflow with either a ≥3% desaturation or an EEG arousal. Obstructive apnoeas were defined as events with a >90% reduction in airflow with maintained respiratory movements. Central apnoeas were defined as events with a >90% reduction in airflow with a cessation of respiratory movements. Mixed apnoeas were defined as events with features of both central and obstructive apnoeas.

Patients subsequently attended two overnight physiological studies to measure loop gain and other physiological traits (e.g. upper airway collapsibility, arousal threshold and upper airway muscle responsiveness) by manipulating CPAP pressure [1, 4]. On both nights, CPAP was dropped from a therapeutic level for 3 minute periods repeatedly during non-REM sleep in order to lower ventilation and provide a *ventilatory disturbance.* Once breathing was constant and below eupnoea, CPAP was switched back to the therapeutic level and the *ventilatory response* (i.e. the overshoot in ventilation above eupnoea) was observed. For each patient, a ventilatory control model (gain, time-constant, delay), of the same basic form used for our new method, was fit to the ensemble-averaged CPAP-drop data to provide a measure of loop gain.

Measurement of airway anatomy/collapsibility. The method to estimate loop gain using CPAP drops also provided two published measures of airway anatomy/collapsibility. The critical collapsing pressure P_{crit} is taken as the x-intercept of a plot of peak inspiratory flow at the onset of abrupt drop (breaths 3-5) in mask pressure, across multiple acute pressure drops. P_{crit} represents the critical level of airway pressure that closes the airway [22]. $V_{passive}$ is the y-intercept of a plot of ventilation (tidal volume × respiratory frequency) at breaths 3-4 after the drop against mask pressure [4]. When ventilation is normalised using eupneic ventilation, $V_{passive}$ represents the proportion of baseline ventilation (on optimal CPAP) than can be achieved through a maximally-passive airway when CPAP is switched off.

Detecting a Lowered Loop Gain with Oxygen and Acetazolamide

We applied our new method to the polysomnographic recordings of patients examined at baseline and following oxygen treatment [23], to determine whether our method could detect the known reduction in loop gain with oxygen. Patients also had loop gain estimates made with 'proportional assist ventilation' method on a separate study night to confirm a reduction in loop gain. Unfortunately, not all polysomnographic data could be obtained from the prior study [23] due to stored file corruption (N=3/12). However, we included unpublished polysomnographic data from two subjects who had been studied on polysomnographic nights (baseline and oxygen) but had not attended for loop gain measurement via proportional assist ventilation.

We also applied our method to the polysomnographic recordings from a cross-over physiological study examining changes in loop gain following acetazolamide [1]. We aimed to assess whether our method could detect the known reduction in loop gain with acetazolamide. Patients had also had loop gain estimates made with the 'CPAP-drop' method to confirm a reduction in loop gain

on a separate study night. In both oxygen and acetazolamide studies, polysomnography was performed at the same laboratory and under the same conditions as described above. Patients provided written informed consent. All studies were approved by the Partners Institutional Review board.

Data Analysis

Recordings and scored events were exported from the polysomnography software (Alice Sleepware, Respironics) as European data format (.edf) and comma separated variable (.csv) files respectively, before being imported and analyzed using in house built MATLAB software.

Choice of window length. Seven-minute epochs of supine non-REM sleep with ≥1 respiratory event were identified using a sliding window with 2 min overlap. The 7 min duration was chosen to provide sufficient time for ~10 cyclic obstructive events (based on the average inter-event interval of ~40 s) which was considered sufficient data for separating chemical drive and arousal contributions to total ventilatory output. Our choice was also influenced by the following considerations: Long periods of sleep are less frequent than shorter ones; thus the requirement for long windows may bias the analysis towards periods of more stable sleep. Longer windows are more likely to suffer from issues of non-stationarity than shorter windows; for example, the relationship between nasal pressure and true flow can change over time with movement. Shorter windows may not contain sufficient information to separate arousal (non-chemical) effects from chemical drive effects on the ventilatory pattern. To confirm that the selected window length was appropriate, a sensitivity analysis was conducted, whereby the key outcome measurements (LG_1, LG_2 and $LG_{1/6}$) were calculated at window lengths of 4, 5, 6, 7, 8, 9 and 10 minutes.

Linearisation of nasal pressure. To provide a linear surrogate of ventilatory flow, we used the square root transform of the nasal pressure signal because the amplitude of the nasal pressure signal is known to be approximately proportional to the square of ventilatory flow [24, 25]. This linearised nasal pressure signal was then treated as an uncalibrated ventilatory flow signal, and was subsequently integrated breath-by-breath to provide a time series of ventilation data (uncalibrated tidal volume × respiratory rate). These ventilation data were then normalised for subsequent analysis (mean ventilation = 1.0, apnoea = 0). Finally, the data were mean subtracted for model analysis (mean ventilation = 0, apnoea = −1.0), since the model equations for chemical drive (Equations 2, S1, S5) describe the changes in ventilatory drive from the mean level. The traces presented (Figure 2a, Figure 3a-b) illustrate values of ventilation and ventilatory drive that are not mean subtracted (the mean is added back to the original data, following analysis, for the purpose of presentation).

Scoring of arousals and obstructed breaths. Using manually scored EEG arousals, a categorical breath-to-breath time series of arousals (Ar=1 or Ar=0, see Equation S4) was created based on whether an EEG arousal is observed within the margins of the breath (Ar=1) or not (Ar=0). Likewise, unobstructed breaths (W=1 or W=0, see Equation S7) were taken as those breaths that were not entirely within the margins of scored obstructive events by a sleep technologist. To account for minor imprecision in the scored timing of respiratory events, we employed the following routine: If the first or last obstructed breaths of scored obstructive event had ventilation > mean ventilation (V_E>1), that breath was considered ‘unobstructed’, and breaths next to a scored event with ventilation<70% mean (V_E<0.7) were considered obstructive. This modification routine was applied iteratively to each scored obstructive event until no further

breaths were modified. Breaths with reduced ventilation but with a parallel reduction in both respiratory and abdominal belt excursions of at least the same magnitude were also taken as 'unobstructed' (indicating that the reduced ventilation is the consequence of reduced ventilatory drive).

Use of first half of the night data for CPAP drop comparison. For the best comparisons with loop gain measured from CPAP drops (taken over approximately the first 4-5 hours of sleep), we used the first 50% of the available polysomnographic data to control for expected time of night effects. The use of data from the first half of the night was also designed to minimise the confounding effect of cyclic OSA and its sequellae (intermittent hypoxemia, sympathoexcitation, sleep deprivation) on measures of control of breathing [26-28] since CPAP drops were performed in the background of an absence of OSA-related sequellae. Patients were compliant CPAP users and on optimum CPAP immediately prior to each drop used to measure loop gain (CPAP drop method).

Associations with loop gain from CPAP drops (Figure 3a-c of the main document) remained significant when polysomnographic data from the whole night were used (LG_1, R=0.54, P=0.003; LG_2, R=0.53, P=0.004; $LG_{1/6}$, R=0.58, P=0.001). Likewise, key correlates between our measure of loop gain (LG_1) and clinical data (AHI, inter-event interval, hyperpnoea interval) remained significant even when data from only the first half of the night were used (AHI, R=0.52, P=0.005; inter-event interval, R=−0.56, P=0.002; hyperpnoea interval, R=−0.61, P=0.001). The relationship between LG_1 and REM−non-REM AHI was no longer statistically significant when data from only the first half of the night were used, although the trend remained (R=−0.34, P=0.08).

SUPPLEMENTAL RESULTS

Loop Gain Quantification in OSA: Comparison to Published Standard

Detailed ventilatory control data from our method are provided in Table S1.

Variability within subjects. The coefficient of variation of loop gain measurements (LG_1) within each patient was 36±9% (N=28), yielding a standard error of 6±2%. Thus, on average, the 95% confidence in each patient's loop gain measurement was ±12% of the reported value.

Comparison at multiple frequencies. Our method yielded values of loop gain that are highly comparable with those taken from the CPAP drop method. However, we note that values tended to be higher when measured from polysomnography compared with the CPAP-drop method, by 20% at 1 cycle/min, and by 20-40% across the frequency range assessed (see Figure S3). It is possible that a decrease in loop gain with a CPAP-induced increase in lung volume may be responsible for this systematic difference.

Clinical correlates of loop gain. To examine the physiological relationships between apnoea severity and loop gain, we assessed associations between multiple variables (AHI, inter-event interval period, post-event duration) and loop gain measured using our novel method and the CPAP drop method (N=28).

Using both methods, a high loop gain was associated with more severe OSA in the form of a greater AHI (Figure S4a).

It has been previously postulated [29] that non-REM-predominant is a ventilatory control disorder (high loop gain), that improves with REM due to the REM-related reduction in chemosensitivity (and thus loop gain) [30-32]. Indeed there is a relative absence of central sleep apnoea (a high loop gain disorder) in REM compared with non-REM sleep [33, 34]. By contrast, in the absence of a ventilatory control disorder (low loop gain) a greater severity of OSA in REM is expected via the dropout in upper airway muscle tone [35]. As such, we tested whether loop gain (measured during non-REM) would be elevated in patients with non-REM-predominant OSA (i.e. patients whose OSA is more severe in non-REM vs. REM) vs. those with REM-predominant OSA (OSA is more severe in REM vs. non-REM). As expected, we found that loop gain was associated with the change in AHI between REM and non-REM (LG_1 vs. ΔAHI; Figure S4b), a finding that reached significance only with our new measure of loop gain. Use of the ratio of REM AHI to non-REM AHI also yielded similar findings (data not shown).

High loop gain was also associated with a shorter inter-event interval (LG_1 vs. inter-event interval; Figure S4c) as expected based on the concept that a more vigorous response will promote faster transitions between the apnoeic/hypopnoeic phases and hyperpnoea phases of breathing[29, 36]. Median values of inter-event interval (excluding intervals >2 min) are presented. Interestingly, a shorter respiratory event duration was not seen with higher loop gain contrary to expectation [36]. Instead, a reduced hyperpnoea duration was linked with elevated loop gain (Figure S4d), that is, the next event is initiated sooner in patients with higher loop gain.

Possible confounding effect of anatomy. There are a number of possible confounding mechanisms by which a more collapsible upper airway may falsely manifest as a higher loop gain. A more collapsible upper airway may provide more severe airflow obstruction, greater desaturation and hypoxic augmentation of chemoreflex gain [37]. It is also possible that a greater reduction in airflow resistance at the end of events might precipitate a greater ventilatory overshoot [38]. To address this potential concern, we assessed the relationships between our measure of loop gain and measures of upper airway collapsibility (i.e. our functional measure anatomy). There were no significant relationships observed between loop gain (LG_1) and measures of collapsibility (P_{crit}, $V_{passive}$), whether loop gain was measured using polysomnography or CPAP drops (Figure S5a-b). It is therefore unlikely that our measure of loop gain is artificially augmented by a greater severity of upper airway anatomical dysfunction.

Sensitivity of analysis window length: Whist we present results using the chosen window length of 7minutes; we also confirm the appropriateness of this window length though a sensitivity analysis. The correlation between polysomnogram derived loop gain and CPAP drop derived loop gain is relatively insensitive to analysis window lengths between 5 and 7 minutes; and remains statistically significant ($P<0.05$) for window lengths up to 9 minutes (Figure S6a). There is a trend for the mean bias of polysomnogram derived loop gain to decrease with increasing window length (Figrue S5b). The selected window length (7 minutes) provides a good trade-off between correlation and mean-bias of loop gain measurements.

Detecting Reduced Loop Gain with Oxygen

In addition to effects reported in the main document, we also observed an increase in our measure of delay with oxygen (Table S1). This finding is consistent with results from physiological studies [39, 40],

and may result from a reduction in cardiac output [41] or increased chemoreflex time lag via a suppression of the fast-acting carotid bodies [42]. The increased natural cycling period (T_n) associated with oxygen treatment is in concordance with the increased cycle duration of periodic breathing previously documented with this therapy [43].

Detecting Reduced Loop Gain with Acetazolamide

Acetazolamide also significantly increased our measure of delay (Table S1), which may be the direct result of an acetazolamide-induced slowing of the chemoreflex response to CO_2 [44, 45], suppression of the sensitivity of the fast-acting carotid-bodies [46, 47], or an indirect effect of improving oxygenation via its known action as a respiratory stimulant. The increase in natural cycling period (T_n) following acetazolamide treatment matches the previously documented increase in cycle duration of periodic breathing [48].

Further comparisons with published standards: Oxygen and acetazolamide

Oxygen and proportional assist ventilation. Precise values for loop gain could not be obtained in several subjects using proportional assist ventilation (PAV) which lead to our view that we would have insufficient power for a comprehensive comparison between our method and PAV. Therefore, such a comparison was not presented as a primary outcome in the current study. Loop gain was reported using PAV in 9/11 subjects at baseline, and 7/11 at both baseline and oxygen [23], although periodic breathing was induced using PAV in only 8 subjects at baseline and 2 subjects on oxygen. In patients that did not exhibit periodic breathing, the PAV-derived loop gain values represent an upper bound on the intrinsic physiologic value (e.g. if we found that loop gain was <0.5 with PAV then 0.5 was taken as their value for our comparison). Using these upper bounds, the PAV data demonstrated a non-significant trend towards a reduction in loop gain (0.45±0.09 at baseline vs. 0.32±0.02 on oxygen). The reduction in loop gain measured using our new technique (Table S1) was consistent with this trend and our recent observation of reduced loop gain with oxygen using the CPAP drop method [39]. Interestingly, when pooling the baseline and treatment data from the oxygen study we found a modest relationship between our measure of LG_1 and PAV-estimated LG (Figure S7a); such a relationship provides further independent validation of our technique.

Acetazolamide and CPAP-drops. Previously, we observed that acetazolamide reduced loop gain as measured using the CPAP drop method (N=12, 0.60±0.09 vs. 0.35±0.06, p=0.013) [1]. When pooling the baseline and treatment data from the acetazolamide study we found a good relationship between our measure of loop gain (LG_1, using the first 50% of the night's data) and CPAP-estimated loop gain (Figure S7b). This relationship provides further independent validation of our technique.

SUPPLEMENTAL DISCUSSION

Physiological Insights

The current study demonstrated that the loop gain of the ventilatory control can be measured from the spontaneous breathing pattern of OSA. The corollary of this finding is that the patterns of ventilatory overshoot and undershoot underlying spontaneous obstructive events are determined, to a significant extent, by the loop gain of the ventilatory control system. This notion provides novel support for the key role of ventilatory control in the pathogenesis of OSA [1, 23, 49-52]. We also show that the effective suppression of OSA with the lowering of loop gain—with either oxygen or acetazolamide—can be predicted from patient characteristics observed on a polysomnogram prior to intervention: a high loop gain and a fast natural cycling period (manifest as a short inter-event interval). Closely-spaced apneic events have been previously suggested (but never demonstrated) to reflect a ventilatory control contribution to OSA [29].

A high loop gain may also impact the sleep state (non-REM vs. REM) in which OSA is predominant. Patients with non-REM predominant OSA (i.e. OSA improves in REM) have long been thought to have high loop gain [29], given the relative absence of central sleep apnoea (a high loop gain disorder) in REM compared with non-REM sleep [33]. Intuitively, REM should improve high loop gain OSA because the heightened chemoreflexes considered responsible for 'high loop gain OSA' are suppressed in REM sleep [30]. Our study demonstrates that a high loop gain can indeed manifest as non-REM predominant OSA.

Assessment of loop gain from mixed and central events

The patients participating in the current study exhibited predominantly obstructive events. However, in principle, our method should apply to central events and mixed (both central and obstructive) events, as confirmed using the mathematical model (Figure 2b illustrates accurate loop gain estimation even when loop gain is elevated sufficiently as to elicit central and mixed events). An example trace illustrating loop gain measurement from mixed apnoeas is provided in Figure S8.

TABLE S1. VENTILATORY CONTROL MEASURES FROM POLYSOMNOGRAPHY

Variable	Comparative Dataset	Effect of oxygen (O_2)		Effect of acetazolamide (ACZ)	
		Baseline	O_2	Baseline	ACZ
Number of windows analysed	47±4	61±9	47±6	58±6	41±6*
Loop gain, LG_1 (mid frequency)	0.71±0.03	0.77±0.10	0.54±0.04*	0.80±0.06	0.60±0.06*
Loop gain, LG_2 (high frequency)	0.38±0.02	0.41±0.05	0.28±0.02*	0.42±0.04	0.30±0.03*
Loop gain, $LG_{1/6}$ (low frequency)	3.08±0.19	3.38±0.38	2.62±0.24*	3.35±0.21	3.10±0.35
Natural cycling period, T_n (s)	38.9±1.5	37.4±2.4	50.7±3.5*	37.0±2.1	48.5±3.2*
Ventilatory response to arousal, γ	0.43±0.05	0.48±0.09	0.22±0.06*	0.28±0.08	0.14±0.03
Time constant, τ (s)	146±9	137±17	160±10	126±16	156±9
Delay, δ (s)	10.43±0.42	10.15±0.66	13.91±1.09*	10.10±0.51	12.99±1.02*

*p<0.05 baseline versus treatment, paired Student's t-test. Data are presented as mean±SEM. The ventilatory response to arousal γ is presented as a fraction of mean ventilation. LG_x is the loop gain (response:disturbance magnitude) for a *x* cycle/min sinusoidal disturbance.

Figure S1

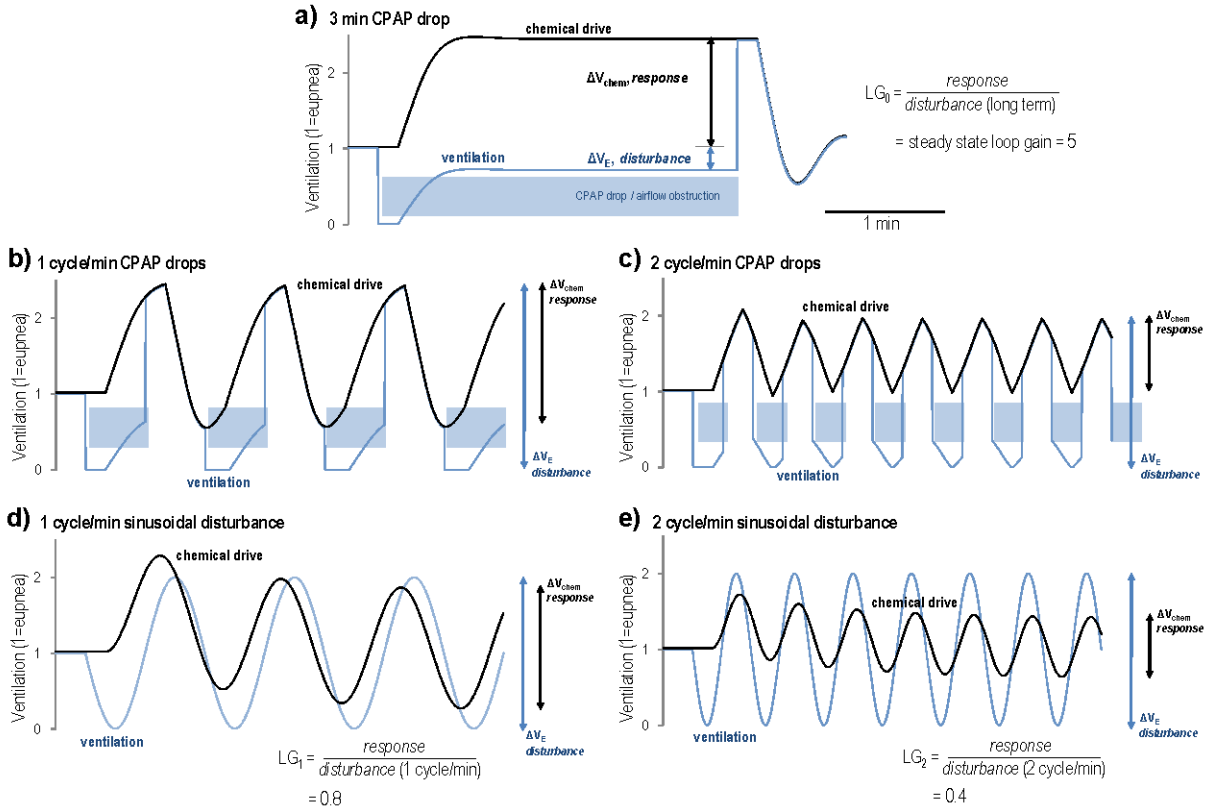

Figure S1. Loop gain varies with the timing of the disturbance: model illustration. Loop gain is defined as the ratio of the change in chemical drive (response) to that in ventilation (disturbance). However, it is less well recognised that loop gain is not simply a single parameter, but instead varies with the timing (frequency) of the disturbance that is considered. The parameters used for this model illustration are as follows: steady-state loop gain (LG_0) = 5 (unitless); time-constant = 1 min; delay = 1/6 min (10 s). (*a*) First consider the long term response to a persistent disturbance (i.e. frequency = 0 cycles/min) that can be measured using continuous positive airway pressure (CPAP) manipulation (drops): First, a reduction in CPAP causes a reduction in ventilation. Some ventilatory compensation is acheived as chemical drive (V_{chem}) increases, and ultimately ventilation lies below the resting level (eupnoea=1) by ΔV_E (the disturbance). Since steady-state loop gain (LG_0)=5, this disturbance provides a chemical drive response that is 5-fold the size of the disturbance, as shown. (*b*) Importantly, the response to a short-term disturbance is not this large, as illustrated by switching CPAP on and off with a frequency of 1 cycle/min (shading denotes reduced CPAP / airflow obstruction). Arrows illustrate the amplitude of the response and the disturbance (at the frequency of the disturbance). In contrast to the steady-state response in (a), the size of the swings in V_{chem} (the response) are now smaller relative to those in V_E (the disturbance) because the full steady-state response has not had time to develop completely before the disturbance changes direction. Panels (*d*) and (*e*) illustrate responses to sinusoidal variation in ventilation, rather than switching CPAP as simulated in (*b*) and (*c*). (*d*) The 1 cycle/min oscillation in chemical drive is 0.8-times the size of the disturbance, such that LG_1=0.8. Without requiring a simulation, we can determine LG_1 from the relationship $LG_1=LG_0/(1+[2\pi\tau f]^2)^{0.5}$. (*e*) At 2 cycles per min, the response is smaller again (LG_2=0.4 in this example). Additional model parameters: acute ΔV_E with CPAP drop at eupnoea=−1.0; compensatory response, $\Delta V_E/\Delta V_{chem}$=+0.5.

Figure S2

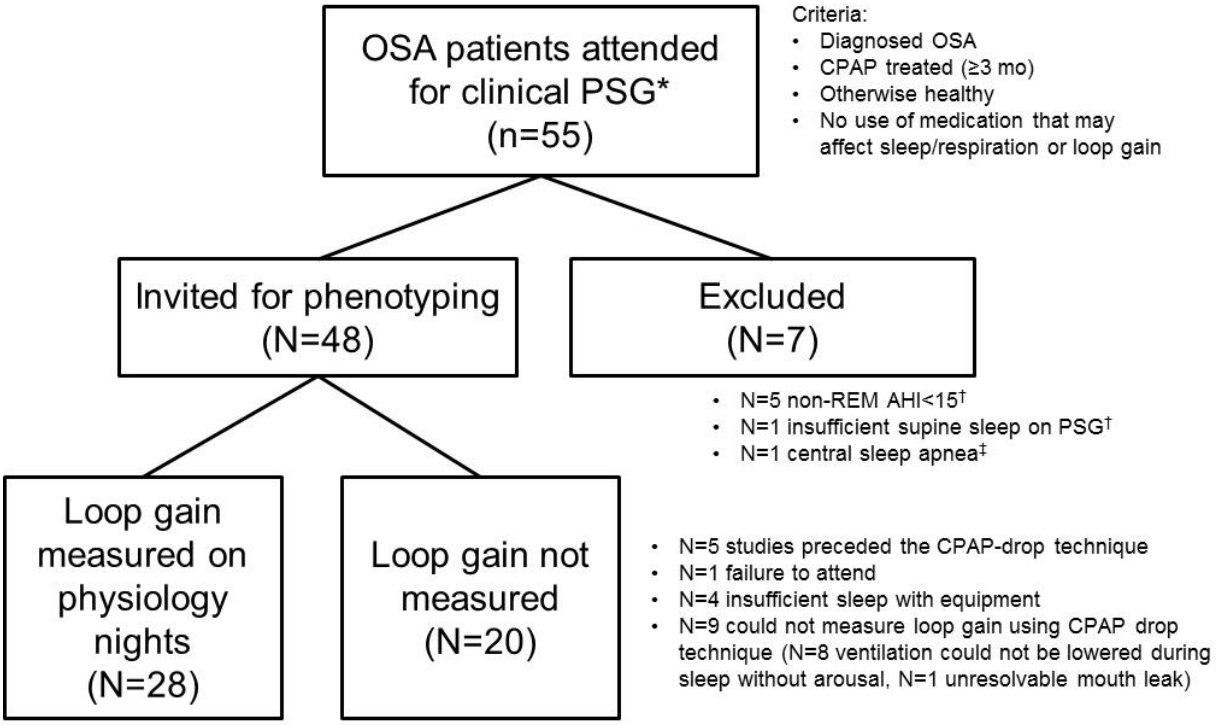

Figure S2. Flowchart outlining the selection of patients for analysis in this study. These patients were drawn from a cohort of patients participating in a study previously published by Eckert et. al. [5]. *Patients with diagnosed and CPAP-treated OSA were invited to attend a clinical laboratory (the former Sleep HealthCenters, MA, USA; Alice Sleepware, Philips Respironics). Later, a further 14 patients with OSA were studied for baseline polysomnography at our physiology laboratory (not included in the current analysis). †Excluded from further analysis in the current study. ‡Excluded altogether from further participation.

Figure S3

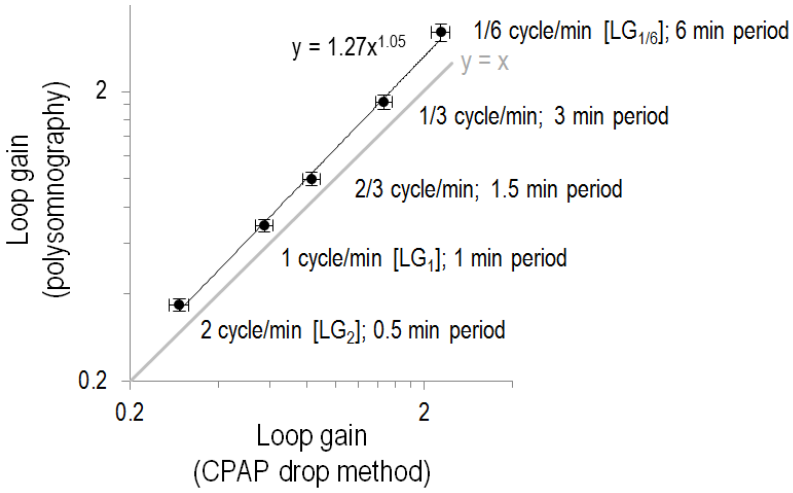

Figure S3. Group data comparison of loop gain between methods across a range of frequencies. Note that at all frequencies shown, our method to estimate loop gain from polysomnography yields values that are ~30% greater than values measured using the CPAP drop method. Data shown are mean±SEM (N=28).

Figure S4

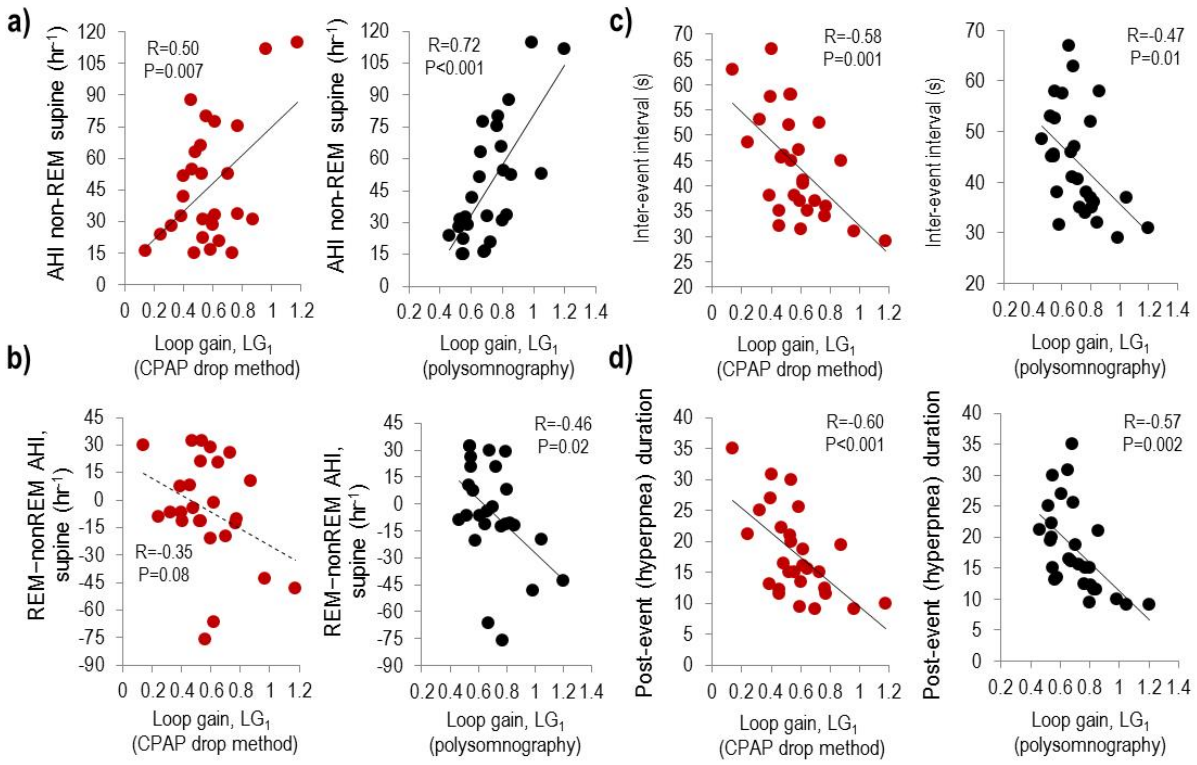

Figure S4. Relationships between clinical variables and loop gain measured using polysomnographic and CPAP drop methods. (*a*) High loop gain is associated with a greater apnoea-hypopnoea index (N=28). (*b*) High loop gain from polysomnography predicts a relative improvement of OSA in REM sleep, a similar trend is seen with such improvement and loop gain measured from CPAP drops (N=26; 2/28 patients had insufficient REM sleep). (*c*) Higher loop gain can be seen in the form of a shorter inter-event interval (reduced duration from one respiratory event to the next), due to (*d*) a reduced hyperpnoea duration (reduced duration from the end of one event to the start of the next) (N=28). Polysomnographically-derived values are taken over the whole night.

Figure S5

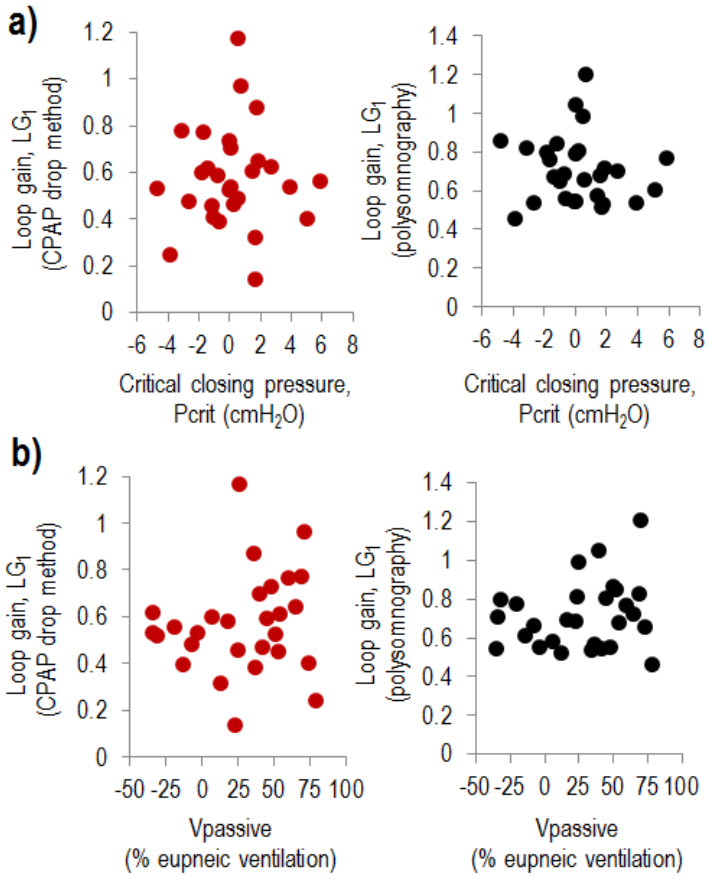

Figure S5. Loop gain measured from polysomnograhy is unlikely to be artificially-increased due to a more compromised anatomy/collapsibility. (*a*) The critical closing pressure (P_{crit}) is the level of CPAP at which the airway collapses completely during sleep. (*b*) $V_{passive}$ represents the ventilation observed when CPAP is acutely switched off during sleep. There is a trend towards a greater loop gain in those with the least compromised anatomy/collapsibility, a finding that was confirmed statistically in the larger dataset for steady-state (zero-frequency) loop gain [5].

Figure S6:

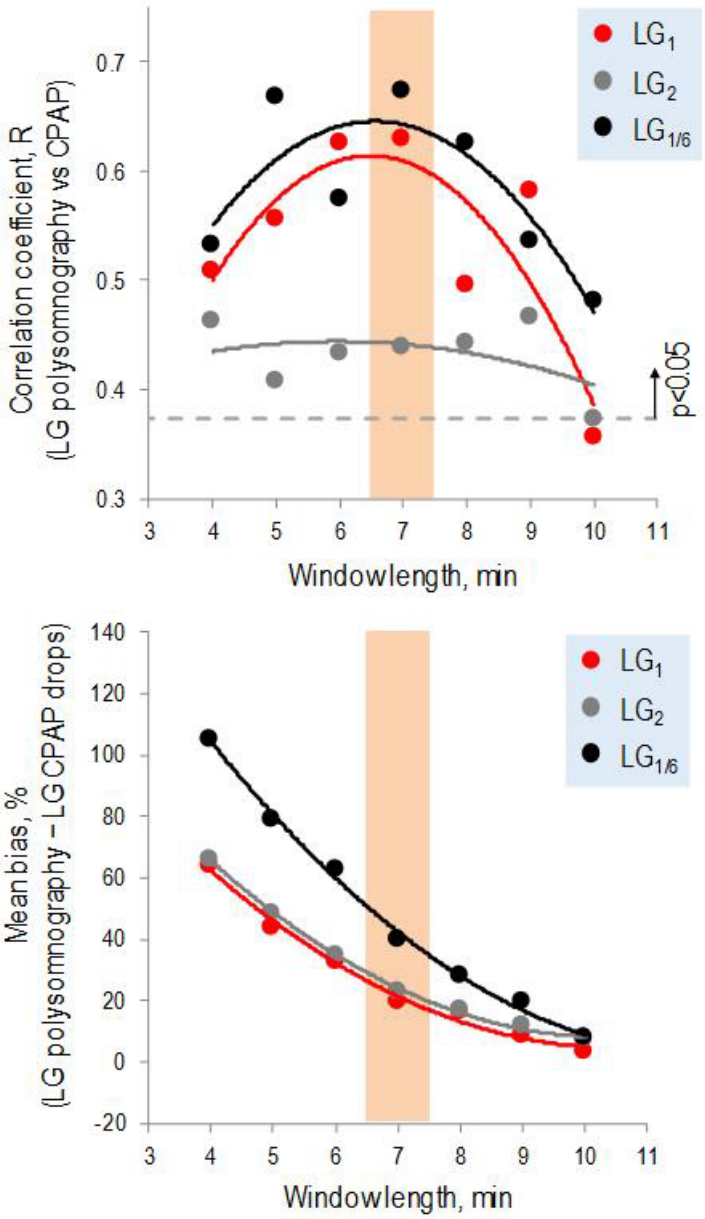

Figure S6 The impact of analysis window lengths on key study outcomes. (a) The correlation between polysomnogram derived loop gain and CPAP drop derived loop gain is relatively insensitive to analysis window lengths between 5 and 7 minutes; and remains statistically significant (P<0.05) for window lengths up to 9 minutes. (b) The mean bias of polysomnogram derived loop gain decreases with increasing window length. The selected window length (7 minutes) provides a good trade-off between correlation and mean-bias of measurements.

Figure S7

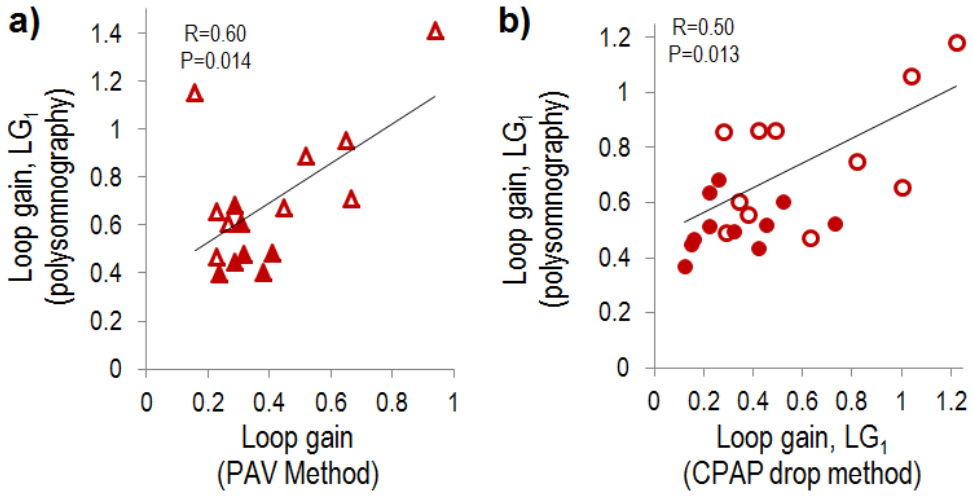

Figure S7. Loop gain estimated from polysomnography agrees with loop gain measured from proportional assist ventilation (*a*) and CPAP drops (*b*). Pooled data include values from baseline studies (open) and treatment studies (solid; oxygen in panel *a*, acetazolamide in panel *b*). Of note, the apparent outlier in panel A (top left; data included in the correlation) exhibited mixed events (27 mixed apnoeas/hr plus 72 obstructive events/hr) at baseline which is consistent with high loop gain (despite low loop gain measured using proportional assist ventilation, PAV). LG_1 denotes loop gain at 1 cycle/min. Loop gain data from polysomnography were taken from the first half of the night.

Figure S8

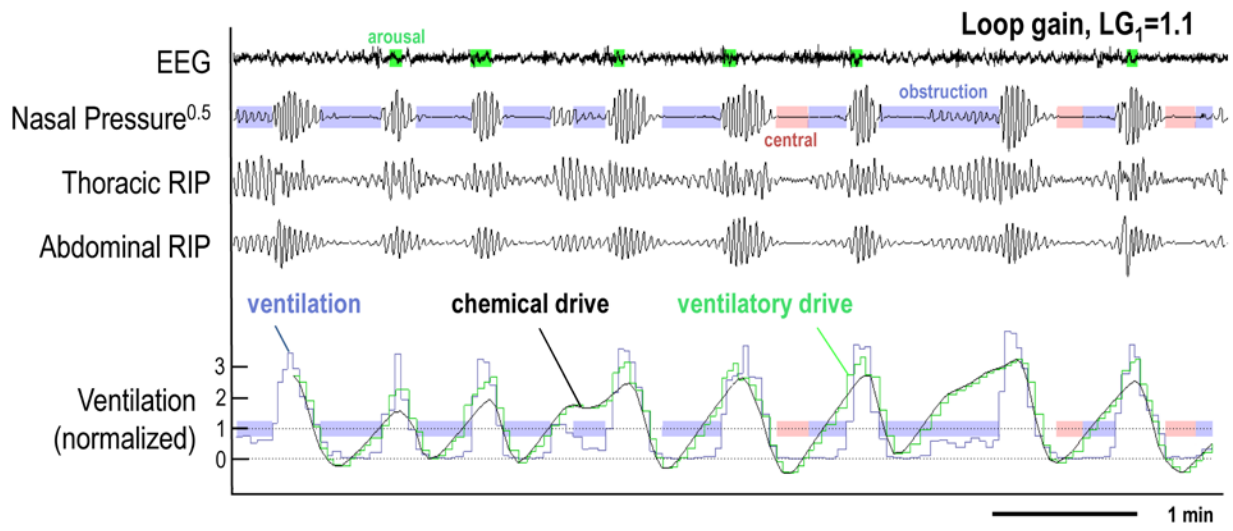

Figure S8 Example epoch of obstructive sleep apnoea with high loop gain and occasional "mixed" events, characterised by a central apnoea [red shaded region] followed by airflow obstruction [blue shaded region]. Note that the estimated chemical drive falls below zero during periods of central apnoea.

SUPPLEMENTAL REFERENCES

1. Edwards BA, Sands SA, Eckert DJ, White DP, Butler JP, Owens RL, Malhotra A, Wellman A. Acetazolamide improves loop gain but not the other physiological traits causing obstructive sleep apnoea. *J Physiol* 2012; 590(Pt 5): 1199-1211.

2. Hall MJ, Xie A, Rutherford R, Ando S, Floras JS, Bradley TD. Cycle length of periodic breathing in patients with and without heart failure. *Am J Respir Crit Care Med* 1996; 154(2 Pt 1): 376-381.

3. Khoo MC, Kronauer RE, Strohl KP, Slutsky AS. Factors inducing periodic breathing in humans: a general model. *J Appl Physiol* 1982; 53(3): 644-659.

4. Wellman A, Eckert DJ, Jordan AS, Edwards BA, Passaglia CL, Jackson AC, Gautam S, Owens RL, Malhotra A, White DP. A method for measuring and modeling the physiological traits causing obstructive sleep apnea. *J Appl Physiol* 2011; 110(6): 1627-1637.

5. Eckert DJ, White DP, Jordan AS, Malhotra A, Wellman A. Defining Phenotypic Causes of Obstructive Sleep Apnea: Identification of Novel Therapeutic Targets. *Am J Respir Crit Care Med* 2013.

6. Trinder J, Ivens C, Kleiman J, Kleverlaan D, White DP. The cardiorespiratory activation response at an arousal from sleep is independent of the level of CO(2). *J Sleep Res* 2006; 15(2): 174-182.

7. Xie A, Wong B, Phillipson EA, Slutsky AS, Bradley TD. Interaction of hyperventilation and arousal in the pathogenesis of idiopathic central sleep apnea. *Am J Respir Crit Care Med* 1994; 150(2): 489-495.

8. Morrell MJ, Harty HR, Adams L, Guz A. Breathing during wakefulness and NREM sleep in humans without an upper airway. *J Appl Physiol (1985)* 1996; 81(1): 274-281.

9. Fink BR. Influence of cerebral activity in wakefulness on regulation of breathing. *J Appl Physiol* 1961; 16: 15-20.

10. Orem J, Osorio I, Brooks E, Dick T. Activity of respiratory neurons during NREM sleep. *J Neurophysiol* 1985; 54(5): 1144-1156.

11. Carley DW, Shannon DC. A minimal mathematical model of human periodic breathing. *J Appl Physiol* 1988; 65(3): 1400-1409.

12. Sands SA, Edwards BA, Kee K, Turton A, Skuza EM, Roebuck T, O'Driscoll DM, Hamilton GS, Naughton MT, Berger PJ. Loop gain as a means to predict a positive airway

pressure suppression of Cheyne-Stokes respiration in patients with heart failure. *Am J Respir Crit Care Med* 2011; 184(9): 1067-1075.

13. Edwards BA, Connolly JG, Campana LM, Sands SA, Trinder JA, White DP, Wellman A, Malhotra A. Acetazolamide attenuates the ventilatory response to arousal in patients with obstructive sleep apnea. *Sleep* 2013; 36(2): 281-285.

14. Khoo MC, Berry RB. Modeling the interaction between arousal and chemical drive in sleep-disordered breathing. *Sleep* 1996; 19(10 Suppl): S167-169.

15. Khoo MC, Koh SS, Shin JJ, Westbrook PR, Berry RB. Ventilatory dynamics during transient arousal from NREM sleep: implications for respiratory control stability. *J Appl Physiol* 1996; 80(5): 1475-1484.

16. Khoo MC, Shin JJ, Asyali MH, Kim TS, Berry RB. Ventilatory dynamics of transient arousal in patients with obstructive sleep apnea. *Respir Physiol* 1998; 112(3): 291-303.

17. Younes M. Role of arousals in the pathogenesis of obstructive sleep apnea. *Am J Respir Crit Care Med* 2004; 169(5): 623-633.

18. Khoo MCK. Nonlinear analysis of physiological control systems. In: Herrick RJ, editor. Physiological control systems Analysis, simulation, and estimation. New Jersey: John Wiley & Sons, Inc.; 2000. p. 229-269.

19. Khoo MCK. Identification of Physiological Control Systems. In: Herrick RJ, editor. Physiological control systems Analysis, simulation, and estimation. New Jersey: John Wiley & Sons, Inc.; 2000. p. 159-202.

20. Manisty CH, Willson K, Wensel R, Whinnett ZI, Davies JE, Oldfield WL, Mayet J, Francis DP. Development of respiratory control instability in heart failure: a novel approach to dissect the pathophysiological mechanisms. *J Physiol* 2006; 577(Pt 1): 387-401.

21. Francis DP, Willson K, Davies LC, Coats AJ, Piepoli M. Quantitative general theory for periodic breathing in chronic heart failure and its clinical implications. *Circulation* 2000; 102(18): 2214-2221.

22. Jordan AS, Wellman A, Edwards JK, Schory K, Dover L, MacDonald M, Patel SR, Fogel RB, Malhotra A, White DP. Respiratory control stability and upper airway collapsibility in men and women with obstructive sleep apnea. *J Appl Physiol* 2005; 99(5): 2020-2027.

23. Wellman A, Malhotra A, Jordan AS, Stevenson KE, Gautam S, White DP. Effect of oxygen in obstructive sleep apnea: role of loop gain. *Respir Physiol Neurobiol* 2008; 162(2): 144-151.

24. Thurnheer R, Xie X, Bloch KE. Accuracy of nasal cannula pressure recordings for assessment of ventilation during sleep. *Am J Respir Crit Care Med* 2001; 164(10 Pt 1): 1914-1919.

25. Farre R, Montserrat JM, Navajas D. Noninvasive monitoring of respiratory mechanics during sleep. *Eur Respir J* 2004; 24(6): 1052-1060.

26. Loewen A, Ostrowski M, Laprairie J, Atkar R, Gnitecki J, Hanly P, Younes M. Determinants of ventilatory instability in obstructive sleep apnea: inherent or acquired? *Sleep* 2009; 32(10): 1355-1365.

27. Salloum A, Rowley JA, Mateika JH, Chowdhuri S, Omran Q, Badr MS. Increased propensity for central apnea in patients with obstructive sleep apnea: effect of nasal continuous positive airway pressure. *Am J Respir Crit Care Med* 2010; 181(2): 189-193.

28. Mahamed S, Hanly PJ, Gabor J, Beecroft J, Duffin J. Overnight changes of chemoreflex control in obstructive sleep apnoea patients. *Respir Physiol Neurobiol* 2005; 146(2-3): 279-290.

29. Thomas RJ, Terzano MG, Parrino L, Weiss JW. Obstructive sleep-disordered breathing with a dominant cyclic alternating pattern--a recognizable polysomnographic variant with practical clinical implications. *Sleep* 2004; 27(2): 229-234.

30. Douglas NJ, White DP, Weil JV, Pickett CK, Zwillich CW. Hypercapnic ventilatory response in sleeping adults. *Am Rev Respir Dis* 1982; 126(5): 758-762.

31. Douglas NJ, White DP, Weil JV, Pickett CK, Martin RJ, Hudgel DW, Zwillich CW. Hypoxic ventilatory response decreases during sleep in normal men. *Am Rev Respir Dis* 1982; 125(3): 286-289.

32. White DP, Douglas NJ, Pickett CK, Weil JV, Zwillich CW. Hypoxic ventilatory response during sleep in normal premenopausal women. *Am Rev Respir Dis* 1982; 126(3): 530-533.

33. Szollosi I, Roebuck T, Thompson B, Naughton MT. Lateral sleeping position reduces severity of central sleep apnea / Cheyne-Stokes respiration. *Sleep* 2006; 29(8): 1045-1051.

34. Zielinski J, Koziej M, Mankowski M, Sarybaev AS, Tursalieva JS, Sabirov IS, Karamuratov AS, Mirrakhimov MM. The quality of sleep and periodic breathing in healthy subjects at an altitude of 3,200 m. *High Alt Med Biol* 2000; 1(4): 331-336.

35. Wiegand L, Zwillich CW, Wiegand D, White DP. Changes in upper airway muscle activation and ventilation during phasic REM sleep in normal men. *J Appl Physiol* 1991; 71(2): 488-497.

36. Younes M. Contributions of upper airway mechanics and control mechanisms to severity of obstructive apnea. *Am J Respir Crit Care Med* 2003; 168(6): 645-658.

37. Lloyd BB, Jukes MG, Cunningham DJ. The relation between alveolar oxygen pressure and the respiratory response to carbon dioxide in man. *Q J Exp Physiol Cogn Med Sci* 1958; 43(2): 214-227.

38. Cistulli PA, Sullivan CE. Pathophysiology of sleep apnea. In: Saunders NA, Sullivan, C.E., editor. Sleep and Breathing. 2nd ed. New York: Marcel Dekker; 1994. p. 405–448.

39. Edwards BA, Sands SA, Owens RL, Hess LB, Smales E, White DP, Malhotra A, Wellman A. Effects of hyperoxia and hypoxia on the physiological traits responsible for obstructive sleep apnea [Abstract]. *Am J Respir Crit Care Med* 2013; 187: A5764.

40. Xie A, Skatrud JB, Puleo DS, Dempsey JA. Influence of arterial O2 on the susceptibility to posthyperventilation apnea during sleep. *J Appl Physiol* 2006; 100(1): 171-177.

41. Haque WA, Boehmer J, Clemson BS, Leuenberger UA, Silber DH, Sinoway LI. Hemodynamic effects of supplemental oxygen administration in congestive heart failure. *J Am Coll Cardiol* 1996; 27(2): 353-357.

42. Carroll JL, Canet E, Bureau MA. Dynamic ventilatory responses to CO2 in the awake lamb: role of the carotid chemoreceptors. *J Appl Physiol (1985)* 1991; 71(6): 2198-2205.

43. Berssenbrugge A, Dempsey J, Iber C, Skatrud J, Wilson P. Mechanisms of hypoxia-induced periodic breathing during sleep in humans. *J Physiol* 1983; 343: 507-526.

44. Tojima H, Kuriyama T, Fukuda Y. Delayed ventilatory response to CO2 after carbonic anhydrase inhibition with acetazolamide administration in the anesthetized rat. *Jpn J Physiol* 1988; 38(1): 55-65.

45. Coates EL, Li AH, Nattie EE. Acetazolamide on the ventral medulla of the cat increases phrenic output and delays the ventilatory response to CO2. *J Physiol* 1991; 441: 433-451.

46. Teppema LJ, Dahan A. Low-dose acetazolamide reduces the hypoxic ventilatory response in the anesthetized cat. *Respir Physiol Neurobiol* 2004; 140(1): 43-51.

47. Teppema LJ, Dahan A, Olievier CN. Low-dose acetazolamide reduces CO(2)-O(2) stimulus interaction within the peripheral chemoreceptors in the anaesthetised cat. *J Physiol* 2001; 537(Pt 1): 221-229.

48. Nussbaumer-Ochsner Y, Latshang TD, Ulrich S, Kohler M, Thurnheer R, Bloch KE. Patients with obstructive sleep apnea syndrome benefit from acetazolamide during an altitude sojourn: a randomized, placebo-controlled, double-blind trial. *Chest* 2012; 141(1): 131-138.

49. Wellman A, Jordan AS, Malhotra A, Fogel RB, Katz ES, Schory K, Edwards JK, White DP. Ventilatory control and airway anatomy in obstructive sleep apnea. *Am J Respir Crit Care Med* 2004; 170(11): 1225-1232.

50. Hudgel DW, Gordon EA, Thanakitcharu S, Bruce EN. Instability of ventilatory control in patients with obstructive sleep apnea. *Am J Respir Crit Care Med* 1998; 158(4): 1142-1149.

51. Sforza E, Boudewijns A, Schnedecker B, Zamagni M, Krieger J. Role of chemosensitivity in intrathoracic pressure changes during obstructive sleep apnea. *Am J Respir Crit Care Med* 1996; 154(6 Pt 1): 1741-1747.

52. Xie A, Bedekar A, Skatrud JB, Teodorescu M, Gong Y, Dempsey JA. The heterogeneity of obstructive sleep apnea (predominant obstructive vs pure obstructive apnea). *Sleep* 2011; 34(6): 745-750.